Permanent Hydrophobic Coating of Chitosan/Cellulose nanocrystals Composite Film by Cold Plasma Processing

Ana Oberlintner[a,b], Alenka Vesel[c], Katerina Naumoska[d], Blaž Likozar[a], Uroš Novak[a,*]

[a] *Department of Catalysis and Chemical Reaction Engineering, National Institute of Chemistry, Hajdrihova 19, SI-1000 Ljubljana, Slovenia*
[b] *Jožef Stefan International Postgraduate School, Jamova cesta 39, SI-1000 Ljubljana, Slovenia*
[c] *Department of Surface Engineering, Jožef Stefan Institute, Jamova cesta 39, SI-1000 Ljubljana, Slovenia, Jožef Stefan Institute, Jamova cesta 39, SI-1000 Ljubljana, Slovenia*
[d] *Department of Analytical Chemistry, Laboratory for Food Chemistry, National Institute of Chemistry, Hajdrihova 19, SI-1000 Ljubljana, Slovenia*

Abstract

A highly effective ultrafast chemical modification of chitosan/cellulose nanocrystals composite film surface is presented in the present research. Added value properties were achieved by the use of a few second's treatment with RF-generated low-temperature fluorocarbon plasma. Drastic increase of the water-repelling character of the completely natural-based biocomposite foil were observed, with contact angle reaching up to 121°. Surface fluorination occurred through formation of irreversible fluorine-related bonds (CF-CF_2, CF_2-CF_2 and C-CF, CF_3 and O-CF_2, O-CF_3) detected by the means of X-ray photoelectron spectroscopy. Surface structural changes were fur-

*Corresponding author
Email address: uros.novak@ki.si (Uroš Novak)

ther confirmed with ATR-FTIR. With packaging application in mind, the films were subjected to analysis of mechanical and water-related properties, showing an improvement upon fluorination. Further the stability of the modification was followed by measurements of water contact angle and atomic composition, as well as mechanical properties, water content and water vapour transmission after at least 31 days of storage in controlled environment. Lastly, no leaching of fluorinated components into liquid environments was detected by the means of HILIC LC-MS analyses in ESI(+) and ESI(-) modes. The presented method rapidly enhances the hydrophobic character of chitosan/nanocellulose biocomposite films without receding mechanical strength and provides a long-lasting surface coating.

Keywords: Chitosan/Cellulose nanocrystals film, Biocomposite packaging, Functionalization with cold plasma processing, Permanent hydrophobic Coating, Shelf-life of modification

1. Introduction

An alarming amount of plastic packaging is produced and discarded every year. Worldwide manufacture of plastic reached 368 million tonnes in 2019, with packaging sector taking up 39.6 % of overall demand [1]. Plastic intended for packaging also has the shortest life cycle with average of only one year and includes non-recyclable plastics such as LDPE and PS [1, 2]. Additionally, the conventional plastic is based on non-renewable resources, which emphasizes the need for an alternative even further.

Chitosan, obtained by deacetylation of chitin, that is found in food-processing industry waste, is one of the promising sustainable materials of the future [3]. Owing to its film-forming ability, focus on chitosan-based films as a potential packaging material is emerging. Besides being non-toxic, bio-compatible and biodegradable, these films exhibit not only sufficient mechanical strength and elasticity, but also antioxidant and antimicrobial properties [4, 3, 5]. Furthermore, the desired characteristics can be tuned by incorporation of various additives, namely plant extracts [6, 7, 8], essential oils [9, 10, 11] into chitosan matrix and was proven to extend the shelf life of various fresh foods [12, 13]. Mechanical properties can be improved by incorporation of cellulose nanocrystals, rod-like shaped nanoparticles isolated from cellulose, the most abundant polymer on earth [14].

Yet, one of the crucial roles of packaging is to protect its content from environmental factors, hence water resistance and low water vapor transmission are desired. Chitosan film exhibits poor moisture barrier, which limits

its wider use [15]. For reference, LDPE, PVC and PLA transmit 1.5 g m^{-2}, 3 g m^{-2} and 40 g m^{-2} of water vapor daily, respectively, while chitosan water vapor transmission rate is as much as 150 g m^{-2} day^{-1} [16]. To tackle this drawback, two approaches of film modification have been researched: i- introducing hydrophobic components such as fatty acids into a film-forming solution [17, 18, 19], or ii- chemically modify polysaccharide [17], while modification of the bio-polymer itself before obtaining a film-forming solution was generally shown not to be suitable, as these derivates often do not exhibit film-forming properties [17]. The first described path to hydrophobization of chitosan leads to composite materials derived from emulsion which can negatively influence other properties, or to multilayer materials [17, 18]. For chemical modification of chitosan surface, various polymer grafting paths were proposed. Up to date literature describes grafting of N-acetyl cysteine to chitosan (resulted in hydrated films with improved tensile properties) [20], alkyl chains to chitosan with intention to improve water resistance for bonding applications [21] and grafting of poly(2-hydroxyethyl methacrylate) chains on chitosan followed by esterification with a fluorinated compound, which is responsible for hydrophobicity [15]. In the latter, the rise in contact angle was 16° and was stable through 10 min of wetting. The drawback of such modification is that the process involves several steps, can be quite time-consuming and produce liquid chemical waste. On the contrary, plasma processing is a single-step modification, eliminating subsequent separation techniques and producing no liquid discard. RF-generated plasma is a mul-

tifunctional tool for etching of the surface or plasma-enhanced chemical vapor deposition, with thermal energy of the electrons being few eV, bringing the atoms to excited state and inducing chemical reaction. Still, the temperature of the electron gas remains low (near room-temperature), allowing modifications of sensitive surfaces, such as biopolymers [22, 23]. The closed reactor system offers the possibility of gas capturing and recycling, preventing harmful gas exhaust into the environment [24, 25]. Furthermore, the possibility of scale-up and utilization of the same assembly system for tailoring the materials surface properties with various dopants (nitrogen, oxygen, sulfur, or fluorine) highlights the industrial applicability of the technique [26, 27, 28].

Despite simplicity, effectiveness and rapidity of plasma treatment, only limited amount of studies concerning chitosan surface functionalization are taking this approach. Several researchers treated chitosan with argon plasma yielding a more hydrophilic surface required in adhesives and coatings, but is not desired for packaging [29, 30, 31, 19]. Slight increase in hydrophobicity, water contact angle rose from initial 13° to 23°, was achieved with alkane vapor plasma technique [32]. On the example of cellulose textiles and films, it has already been demonstrated that plasma using fluorinated compounds as a carrier gas successfully modifies surface and enhances its hydrophobic character [33, 34, 35, 36, 28].

Chow et al. [37] reported general non-cytotoxicity of fluorinated chitin derivates, leading to increased interest in use of these materials as wound dressing agents or topical medication, taking in advantage their antibacte-

rial activity [38, 39]. Furthermore, as demonstrated on example of fluorine-modified cellulose [40], fluorinated biopolymers can be enzymatically degraded by dehalogenases in several microorganisms, that are present in soil and aqueous environment [41, 42].

With respect to these facts, the present study focuses on utilization of RF-generated plasma in fluorocarbon (CF_4) for improvement of water-related properties of chitosan-based films reinforced with cellulose nanocrystals (CNCs) as a fast, efficient, non-destructive and stable modification process, to best of our knowledge, for the first time. The samples were treated for 5 s, which was the optimal treatment time as determined according to water contact angle measurement, and subjected to surface analyses with XPS, FTIR-ATR and SEM. Further, physicochemical properties relevant for packaging application were considered (mechanical properties, moisture content and water vapor transmission. To prove stability of modification, which can be deemed as uncertain, the water contact angle was followed through a period of 40 days, while other properties were re-evaluated after 31 days of storage in controlled environment. Finally, the hydrophobized films stability and possible migration of fluorinated species into liquid environments was examined, to validate applicability of plasma-treated chitosan-based films as packaging.

2. Experimental Section

2.1. Materials

High molecular weight chitosan (85 % deacetylated), lactic acid (85 % aqueous solution) and ammonium formate (for LC-MS) were bought from Sigma-Aldrich (Steinheim, Germany). Cellulose nanocrystals were supplied by Navitas (Stari trg pri Ložu, Slovenia). Glycerol was acquired from Pharmachem Sušnik (Ljubljana, Slovenia), while ethanol (absolute), acetic acid (glacial 100 % and 100 %, for LC-MS) and ammonia solution (32 %) were purchased from Merck (Darmstadt, Germany). Acetonitrile for LC-MS was obtained from Honeywell (North Carolina, USA) and ultrapure water (18 $M\Omega^{-1}$ cm) was supplied by a Milli-Q water purification system (Millipore, Bedford, MA, USA).

2.2. Fabrication of Chitosan-Based Films with Incorporated CNCs

Chitosan-based films were prepared according to a previously described protocol [14]. Detailed description can be found in Appendix A.

2.3. Hydrophobization of Films by Fluorocarbon (CF_4) Plasma Treatment

Chitosan-based films with incorporated CNCs were cut out in different sizes, according to the further analysis. One sample at the time was placed on the microscopic glass and fixed with carbon tape. The sample was then introduced into the 80 cm long discharge tube made of borosilicate glass with diameter 4 cm. The tube was pumped with a two-stage rotary pump

of a nominal pumping speed of 80 m^3 h^{-1}. The base pressure was 1 Pa. Plasma was sustained by a coil with six turns which was connected to the RF generator via a matching network. The generator operated at the standard frequency of 13.56 MHz. The output power was set to 150 W, which was found to be the optimal among preliminary tested 150 W, 200 W and 400 W (data not shown). At these conditions, diffusing plasma expanded far away from the coil. The sample was positioned 7 cm away from the coil. The treatment was carried out with CF_4 gas at 50 Pa for 0.5 s, 1 s, 3 s, 5 s, 10 s, 20 s and 30 s.

2.4. Films Surface Analyses

Water contact angle (WCA), analyzed with Drop Shape Analyser DSA-100 (Krüss GmbH, Hamburg, Germany), was measured at two points in this study: immediately after the treatment on all of the samples and through period of 40 days on the selected sample (treated for 5 s). A static contact angle was determined using a sessile drop method. MiliQ water with the volume of the drop of 1 µL was used for the measurements. The first set of measurements was applied to select the optimal treatment time and the second to follow the effect of aging onto the newly reached hydrophobic character of the surface. The surface chemical composition of the samples was analyzed by means of X-ray Photoelectron Spectroscopy (XPS) using instrument TFA XPS (Physical Electronics, Munich, Germany). Monochromatic Al K$\alpha_{1,2}$ radiation at 1486.6 eV over an area of 400 μm^2 was used as a source

for excitement. Hemispherical analyzer positioned at an angle of 45 ° with respect to the sample surface was applied for the detection of photoelectrons. The survey spectra were measured at a pass energy of 187 eV with an energy step of 0.4 eV. High-resolution XPS spectra of carbon C1s were measured at a pass energy of 29.35 eV with an energy step of 0.125 eV. For surface charge neutralization an additional electron source was used. The C-C component in C1s was set to the binding energy of 284.8 eV. Analysis of the obtained spectra was carried out using MultiPak v8.1c software (Physical Electronics, Munich, Germany). The C1s spectra were fitted with the Gauss-Lorentzian function, where the width and positions of the peaks were fixed during the fitting procedure. FTIR spectra of the untreated samples, treated samples right after the treatment and after 31 days were recorded with ATR-FTIR Spectrum Two (Perkin Elmer, Germany) from 4000 cm^{-1} to 400 cm^{-1} with 4 cm^{-1} step, accumulation of 64 scans. All measurements were done in parallels. Treated and untreated samples were coated with 10 nm layer of gold and were subjected to SEM analysis with Supra 35VP electron microscope (Carl Zeiss, Jena, Germany).

2.5. Film Physico-Chemical Properties

Film thickness and mechanical properties of the film samples were determined according to Bajić et al. (2020), with slight modification in the latter (size of the samples was 6 x 2 cm and gauge length segment was 4 cm). For a detailed description of the analysis the reader is referred to Appendix A.

Protocol described by [5] was followed for assessment of water vapor transmission (WVT). Brief description can also be found in Appendix A. During the aging process the samples were stored at 50 % RH and room temperature.

2.6. Film stability in liquid environments

To observe stability of fluorinated compounds in liquid environments, processed sample was cut into smaller pieces with mass approximately 10 mg and submerged into liquid media (water, 5 % acetic acid$_{(aq)}$, 10 % ethanol$_{(aq)}$) of appropriate volume so the final concentration was 2 mg$_{film}$ mL^{-1}. The samples were collected after 144 h (this time was selected to achieve the longest possible submersion time while avoiding disintegration of the sample, visible after 168 h), dried under nitrogen flow and the solid residues were redissolved in 70 % acetonitrile and analyzed with LC-ESI-MS system in positive and negative ionization mode. UHPLC-MS system (Accela 1250, coupled to an LTQ Velos MS, Thermo Fisher Scientific, Waltham, MA, USA) was used to analyze liquid media upon contact with reference and CF_4 treated films). HILIC LC-MS analyses in ESI(+) and ESI(-) mode were carried out on Phenomenex Luna NH_2 (100 Å, 100 × 2.0 mm i.d., 3 µm) column using 0.05 % ammonia in water solution (mobile phase A) and acetonitrile (mobile phase B) with gradient elution from 10 % to 40 % A in 10 min at a flow rate of 300 μL min^{-1}. Re-equilibration of the column with initial conditions was applied from 11^{th} to 20^{th} min before each next injection. Column oven and autosampler temperature were set at 25 °C and 5 °C, respectively. Injection volume

was 2 μL. Alternative HILIC and RP methods are described in Appendix A. MS parameters were optimized using glucosamine standard (25 μg/mL) and were as follows: heater temperature 300 °C, sheath gas 41 a.u., auxiliary gas 35 a.u., sweep gas to 0 a.u., spray current 5 µA, capillary temperature 200 °C and S-Lens RF Level 49 %. The MS spectra were acquired in the m/z range of 50–2000. The collected chromatograms and spectra were evaluated using the Xcalibur software (version 2.1.0, Thermo Fisher Scientific).

3. Results and Discussion

3.1. Film Surface Analyses

The produced chitosan/cellulose nanocrystals films subjected to CF_4 plasma for various time duration (0.5 s, 1 s, 2 s, 5 s, 10 s, 20 s and 30 s). Water contact angle (WCA), that was evaluated immediately after the treatment, increased abruptly from 94 ± 4 ° to 121 ± 2° in the first two seconds and then stabilized between 122 ° and 125 ° with further processing as shown in Figure 1a. WCA reached with treatment is higher than water repelling of biopolymer films (75 ° for chitosan-only, 58 ° for alginate reinforced with CNCs, 23 ° for cellulose nanofibrils films and around 52 ° for starch film) [14, 43], as well as conventional polymers (PE 102 °, PS 91 °, PVC 87 ° and PET 81 °) [44]. To reveal the cause of this occurrence, the samples were inspected with XPS that showed the saturation of the surface with fluorine in the first two seconds of processing, which correlates to the increase of WCA and its stabilization (Figure1b). The initial C:O:N ratio (69:27:4), was notably altered

upon fluorination. The composition at saturation with fluorine, that is after two seconds of processing, was 41 % carbon, 48 % fluorine, 10 % oxygen and 1 % nitrogen. It was also observed that the ratios slightly change, namely higher carbon, oxygen and nitrogen content and lower fluorine percentage, when plasma is operating longer, which could be attributed to the etching of the surface. Based on these observations, 5 s was chosen as an optimal treatment time and was used for further analyses.

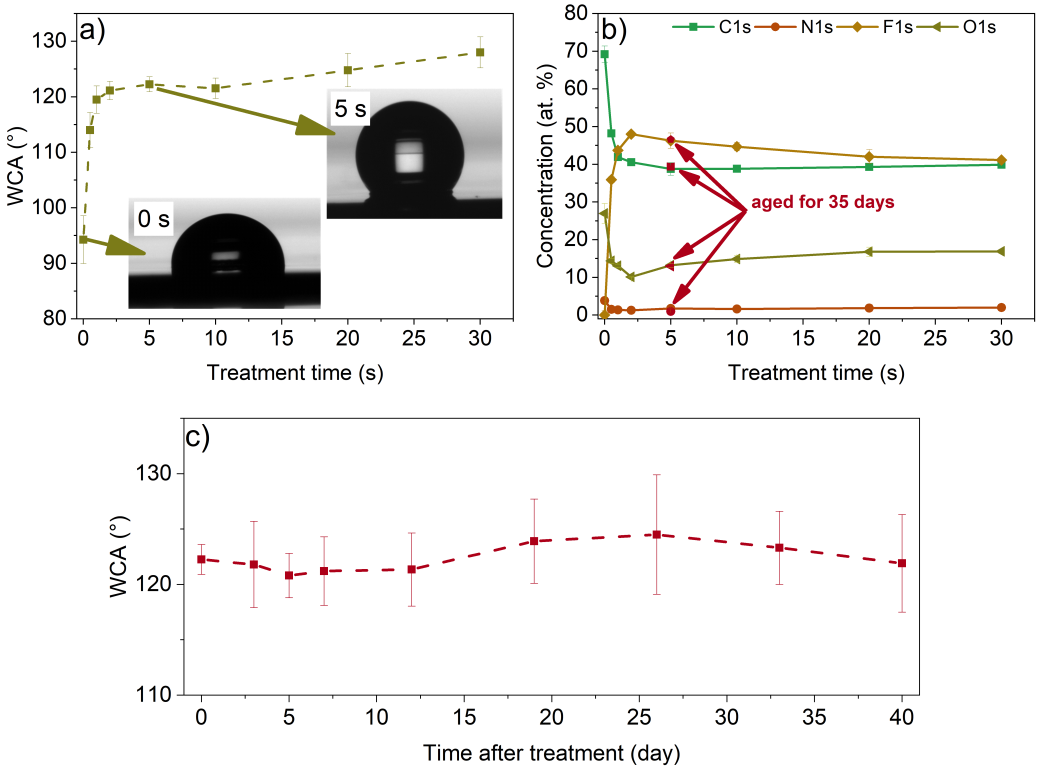

Figure 1: a) WCA of the samples with respect to treatment time, b) atomic composition at various treatment times and atomic composition of the sample treated for 5 s after 35 days (marked in red) and c) stability of WCA over a period of 40 days.

The treated films remained semi-transparent, slightly brown in color and

slightly sticky, indicating that plasma treatment had no effect detected with a naked eye. However, plasma treatment can cause etching on the surface of the film, surface morphology was closely inspected with SEM before and after processing. The micrographs shown in Figure 2 are taken at magnifications 1 k, 10 k and 20 k from left to right. At the smallest magnification, the reference and the treated surface seem smooth with no visible roughness or porosity. Further magnification, however, reveals the structure of rod-like shaped CNCs in the film. The particles seem to be evenly distributed in the chitosan matrix. The surface retained the same morphological properties after the modification.

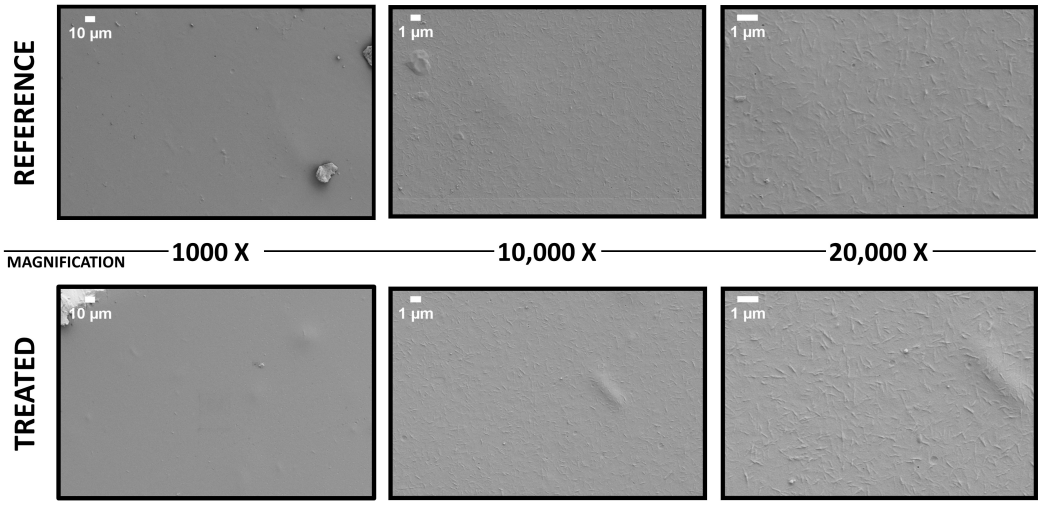

Figure 2: SEM images of reference and treated sample at three different magnifications.

Alternative to conventional polymers used for packaging applications is required to exhibit stable composition and water repelling character over longer period of time. Observations based on the following of WCA over the

period of 40 days showed that it remained constant at around 120 °. Additionally, the composition was shown to remain the same after 35 days of aging with C:F:O:N ratio 39:47:13:1. Hereby, the interest in the surface chemistry throughout the plasma treatment arose, so high-resolution XPS carbon spectra of samples processed for various times were recorded (Figure 3a). To gain a deeper insight into C-F related binding contributions the deconvolution of the C 1s peaks was performed for the reference sample and sample treated for 5 s. In the untreated sample, the C-C (284.8 eV), C-O (286.5 eV), O-C-O (288.0 eV) and O-C=O (289.0 eV) bonds were detected. The intensity of the peak corresponding to initially prevalent C-C bond decreases with plasma processing, while at the same time, peaks related to various C-F bindings start to increase. With longer treatment times the peaks at higher binding energies, that correspond to carbon atoms binding to more than one fluorine, become more prominent. It can be observed that the intensity of the peak at 293.5 eV, corresponding to CF_3 bond, is increasing in the first five seconds of the treatment but this trend takes a turn and the peak starts to decrease with further processing. On the other hand, at the same time, the peak featuring the C-C bond starts to increase after initial decrease in the first 10 s of the treatment that, again, could be due to the etching of the already treated surface and is in alignment with the previously described alteration of atomic ratios. Further, the high-resolution C 1s XPS spectrum of sample treated for 5 s was inspected into detail (Figure 3c). The shape of the treated sample's spectrum differentiates greatly compared to the reference because

of the formation of various fluorine groups. Decrease in the intensity of the initially present peaks corresponding to C-C, C-O and O-C=O bonding was detected, with the latter completely disappearing upon treatment, while the peak positioned at 288.0 eV met a slight increase. However, this same peak can be associated with CF-CF binding as well which is most possibly responsible for the inflation. The treated sample is featured by the newly developed peaks attributed to CF-CF_2 (289.5 eV), CF_2-CF_2 and CF-CF_2 (291.5 eV), CF_3 (293.4 eV) and O-CF_2, O-CF_3 (295.0 eV).

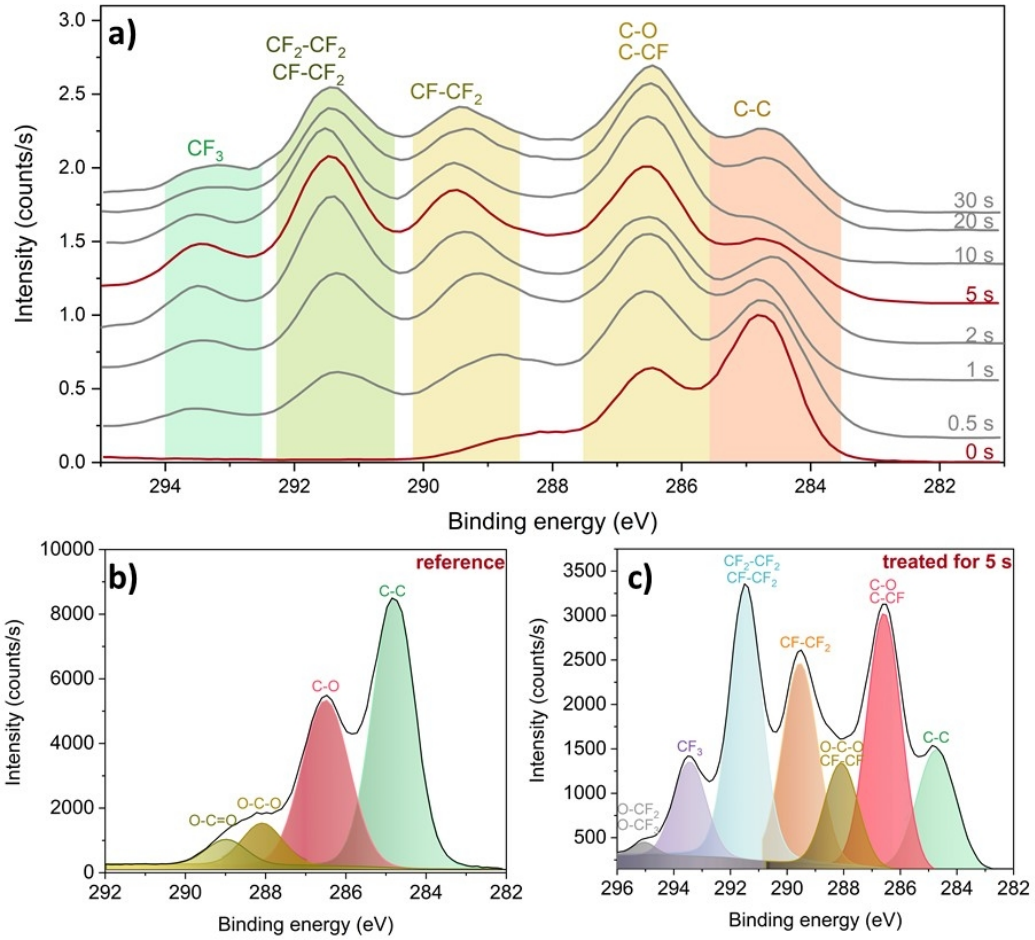

Figure 3: a) Evolution of high resolution XPS carbon spectra according to plasma processing time; b) and c) deconvolution of high-resolution C 1s XPS spectrum of reference material and sample treated for 5 s, respectively.

To further understand possible structural changes upon fluorination, the sample treated for 5 s were additionally analyzed by means of FTIR-ATR and compared to the reference spectrum. Both spectra exhibited characteristic peaks for chitosan namely: the broad peak between 3500 cm^{-1} and 3030 cm^{-1} (corresponds to O-H and N-H bands in chitosan), the two weak bands

located between 2820 cm^{-1} and 3015 cm^{-1} (attributed to C-H stretching in alkane groups), peaks appearing between 1490 cm^{-1} and 1750 cm^{-1} (assigned to C=O stretching - carbonyl and amide I, and N-H bending - amide II, respectively) [45, 46]. The shapes of the treated and non-treated spectra differentiate in the four different regions marked I-IV in Figure 4. The peaks in region positioned between 2830 cm^{-1} and 3000 cm^{-1}, that are attributed to alkane C-H stretching, the absorbance decreases upon plasma processing pointing to lower abundance of these groups. Similar trend is visible in regions II and III, both corresponding to C-O stretching, where the peak positioned at 1287 cm^{-1} disappears and the peaks between 1130 cm^{-1} and 1060 cm^{-1} straighten after fluorine treatment. Similarly, examining region IV, corresponding to C-H bending, it can be observed that the intensity decreases.

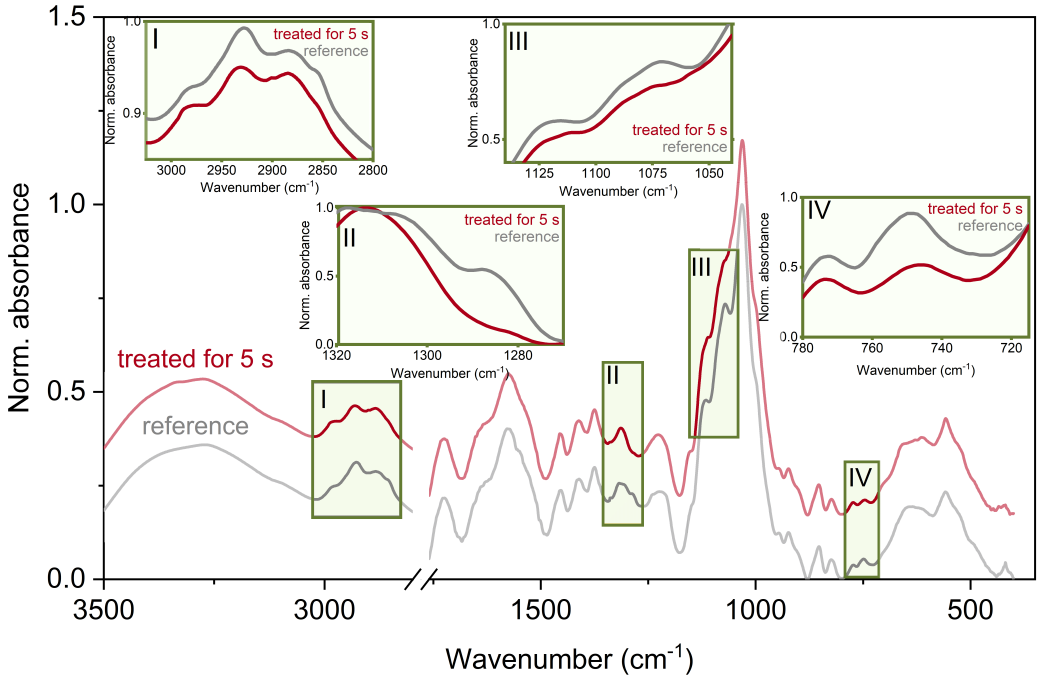

Figure 4: FTIR-ATR spectra of reference and sample treated for 5 s immediately after processing with marked regions where the structural changes were observed.

3.2. Physico-chemical Properties

For packaging important properties, namely tensile strength (TS), elongation at break (ϵ) and water vapor transmission (WVT) were measured immediately after the treatment as well as after 31 days of aging in the controlled environment. As seen in Figure 5, TS and ϵ did not decline with hydrophobization, which was of concern with this treatment. On the contrary, TS improved by 68 % (from initial 1.38 $\pm$ 0.37 MPa to 2.32 $\pm$ 0.51 MPa after the treatment). Similarly, the ϵ increased from the original 63 $\pm$ 13 % to 78 $\pm$ 10 %. It is worth noting, that both of the measured mechanical properties are strongly influenced by the thickness of the film and

moisture content (MC). While the thickness of the films (0.10 ± 0.01 mm) did not deviate upon modification, MC decreased in the fluorinated samples from initial 11.6 ± 0.4 % to 9.2 ± 0.3 %. The water is bound in the sample through hydrogen bonding sites in chitosan (Bajić et al., 2020), so the lower amount of moisture after treatment might be attributed to saturation of hydrogen binding sites of chitosan and CNCs with fluorine. As moisture has a plasticizing effect on the film, TS and MC are in inverse correlation [47], which explains the increase in TS of the treated sample well. However, generally, elongation rate has positive correlation to MC, which is not the case in the fluorinated samples. The newly formed bonds between fluorine and chitosan-CNCs might contribute to higher stiffness of the material. The mechanical properties of biopolymer films strongly relate to free and bound water [7]. Leceta et al. suggest that the water bound inside the crosslinked composite matrix tends to form hydrogen bonds with more polar functional groups, which are in this case the newly added fluorine-related groups on the surface. With this, the internal film structure is damaged, resulting in loss of strength, stiffness and lower stretching [48]. Furthermore, high resolution spectrum of the aged sample was thoroughly inspected (Fig. A2), suggesting that the bonds, disrupted during the aging process, are in the backbone of the polymer chains, which could negatively affect the mechanical properties shown in Figure 5. Aging of the films leads to loss of the advantage in mechanical properties gained by treatment. MC in the reference sample remains constant, whereas in the fluorinated one the moisture content increased to

13 ± 1.0 % and consequently a drop in TS was seen. Based on assumption that the moisture content was lower in the treated film because of formation of hydrogen bonds between chitosan-CNCs and fluorine, the increase over time could be attributed to substitution of these binding with water-chitosan again. Both reference and processed films age into a stiffer material with ϵ 59 ± 14 % and 56 ± 13 %, respectively. Important role of packaging is to shelter the contents from loss of moisture or to prevent the moisture from the environment to breach into the inside and effect the contents. Upon treatment, water vapor transmission (WVT) lowered (from initial 51.3 ± 0.4 g cm^{-2} day^{-1} to 36.5 ± 3.0 g cm^{-2} day^{-1}) as shown in Figure 5, which could be attributed to increase in hydrophobic character. Comparing to other available materials, the processed sample is better at preventing water transmission than PVA, nanocellulose-based films, cellophane and PCL and comparable to PS, Nylon 6 and PLA [16]. With aging, WVT slightly decreases in both samples, with treated sample still performing better than the reference.

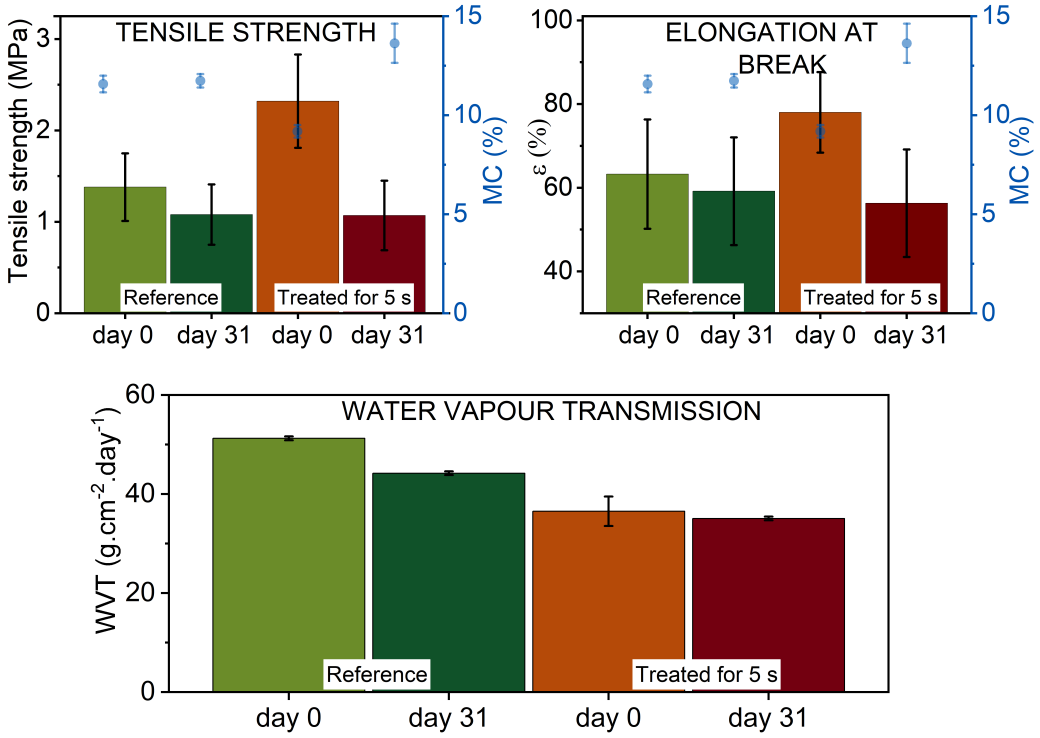

Figure 5: TS, ϵ and WVT of the reference and sample treated for 5 s immediately after processing and after aging in controlled environment for 31 days.

3.3. Film stability in liquid environments

To further demonstrate suitability of the plasma treated material in packaging industry, which was suggested by the measured physicochemical properties and long-term stable hydrophobicity, the interaction of the films with liquid environments was evaluated. The main concern related to material′ s adequacy as packaging is potential leaching of fluorinated compounds into the environment, which was explored with an untargeted analysis of film leachates in water, 5 % acetic acid$_{aq}$, 10 % ethanol$_{aq}$ in both HILIC and RP modes using ESI(+)-MS and ESI(−)-MS. Two HILIC methods and an RP

method were used to analyze the samples. LC-MS chromatograms of treated samples were compared with those of reference (blank) samples to reveal the potential leaching of fluorinated compounds. Both HILIC methods showed comparable results. In RP method, all peaks eluded in dead time (as expected for polar compounds such as glucosamine and N-acetyl glucosamine, potentially present in the simulants as monomer units of chitosan). The experiments showed no difference between the reference and treated sample, except for the water samples (LC-ESI(+)-MS chromatograms and MS spectra shown in Figure 6; supplementary LC-MS chromatograms of the leachates are presented in Fig. A2. In the reference sample, the peak at t_R 6.8 min (marked with I) corresponds to the signal at *m/z* 586, which matches a formula of a trimer consisting of one glucosamine (GlcN) unit and two *N*-acetyl-D-glucosamine (GlcNAc) units. LC-MS analysis of treated water sample showed three split peaks, for which the MS analysis revealed that both parts correspond to the same *m/z*, so the splitting could be attributed to the existence of isomerism or aminosugar anomerism. The peaks with t_Rs between 4.2-5.0 min (peaks III and IV) correlate to *m/z* 180, which is attributed to protonated GlcN. The following two peaks with t_Rs between 5.6-6.0 min (peaks V and VI) and between 6.6-7.2 min (peaks VII and II) correspond to *m/z* at 341 (protonated GlcN/GlcN dimer) and *m/z* at 544 (protonated GlcN/GlcN/GlcNAc trimer), respectively [49]. Additionally, the peak with t_R 6.8 min in the treated sample (peak II) that coincide with the t_R of peak I in the control sample showed additional mass peak of lower

intensity (m/z at 586), which was attributed to GlcN/GlcNAc/GlcNAc [49]. There were no detected peaks pointing to traces of fluorinated compounds in both HILIC and RP using either positive or negative ionization mode, however some limitations apply to this approach. The MS parameters were tuned using glucosamine as a standard due to the non-commercially available fluorinated standards. Moreover, taking into consideration that only surface was modified, it can be assumed that the concentration of potential fluorinated compounds leached into the liquid media is rather low, and may be under the limit of detection (LOD) of our methods, however LODs cannot be calculated due to the absence of standards.

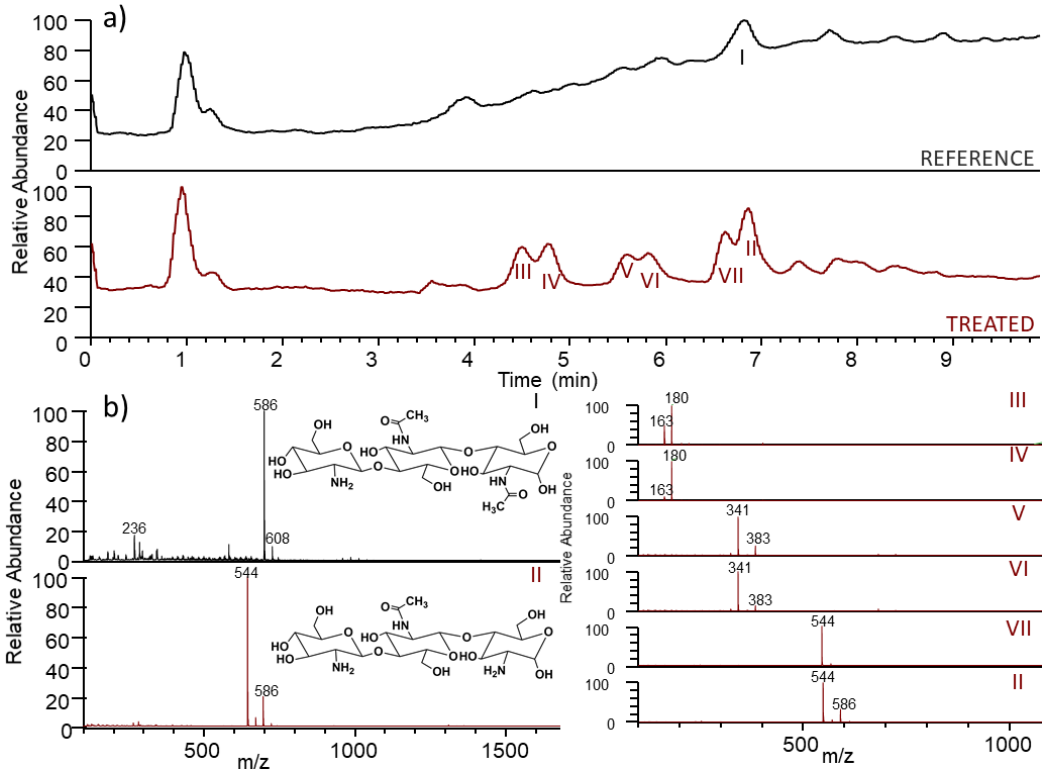

Figure 6: HILIC LC-ESI(+)-MS chromatograms of water leachates in which reference (black) and sample treated for 5 s (red) were submerged for 144 h (a) with marked peaks further analyzed with MS and their corresponding spectra (b).

4. Conclusions

Hydrophobization of bioplastic bio-composite formed from chitosan with incorporated cellulose nanocrystals have been achieved using ultrafast and efficient RF-generated plasma treatment. The main effect of the hydrophobization was to improve water-related properties and raise the material's suitability for packaging applications. After only 5 s of treatment, the increase of WCA by 28° was achieved. The insight into the surface chemistry behind these changes was provided, with XPS revealing newly formed

fluorine-related bonds, while a decrease in C–H and C–O stretching and C-H bending was detected with FTIR-ATR. It is worth noting, that the surface was not damaged by the treatment. Plasma processing decreased MC in the fabricated films, which influenced TS, ϵ and WVT. However, for the role of packaging, the modified sample performed better than the reference one. Stability of the hydrophobic coating, an important aspect for this application, was demonstrated by following WCA over 40 days as well as determining comparable atomic composition with XPS after 35 days of aging. On the other hand, TS, ϵ and WVT all decreased in both, treated and reference sample with time, causing the processed material to lose its superiority. Lastly, to investigate the material's interaction with liquid environments and potential leaching of fluorinated compounds, the films were immersed in three different liquid environments (water, 5% acetic acid, 10% ethanol) and analyzed by means of LC-MS. No evidence pointing to presence of fluorinated compounds were found.

Author Contributions

Oberlintner Ana: Conceptualization, Methodology, Investigation, Data Curation, Writing - Original Draft, Visualization. **Vesel Alenka**: Conceptualization, Methodology, Formal analysis, Investigation, Data Curation, Writing - Original Draft. **Katerina Naumoska**: Methodology, Investigation, Data Curation, Writing - Review & Editing. **Blaž Likozar**: Writing - Review & Editing, Supervision, Project administration, Funding acquisition,

Uroš Novak: Conceptualization, Writing - Review & Editing, Supervision, Project administration, Funding acquisition

Acknowledgements

The authors acknowledge Anže Prašnikar for SEM images. The research was funded by PhD research grant (Ana Oberlintner) and Slovenian Research Agency (ARRS) programs P2-0152, P2-0151 and P1-0005.

References

[1] Plastic Europe - Association of Plastics Manufactures, Plastics – the Facts 2020: An analysis of European plastics production, demand and waste data, Tech. rep., Plastics Europe, Brussels, Belgium (2020).
URL https://www.plasticseurope.org/application/files/3416/2270/7211/Plastics{_}the{_}facts-WEB-2020{_}versionJun21{_}final.pdf{%}0Ahttps://www.plasticseurope.org/en/resources/publications/4312-plastics-facts-2020

[2] Plastic Europe - Association of Plastics Manufactures, Plastics - the Facts 2019: An analysis of European plastics production, demand and waste data, Tech. rep., Plastics Europe, Brussels, Belgium (2019). 10.31025/2611-4135/2019.13894.
URL https://www.plasticseurope.org/application/files/9715/7129/9584/FINAL{_}web{_}version{_}Plastics{_}the{_}facts2019{_}14102019.pdf

[3] Novak, U., Bajić, M., Kõrge, K., Oberlintner, A., Murn, J., Lokar, K., Triler, K. V., Likozar, B., From waste/residual marine biomass to active biopolymer-based packaging film materials for food industry applications – a review, Physical Sciences Reviews. 5 (2020). doi:10.1515/psr-2019-0099.

[4] van den Broek, L. A. M., Knoop, R. J. I., Kappen, F. H. J., Boeriu, C. G., Chitosan films and blends for packaging material, Carbohydrate Polymers. 116 (2015) 237–242. https://doi.org/10.1016/j.carbpol.2014.07.039.

[5] Oberlintner, A., Bajić, M., Kalčikova, G., Likozar, B., Novak, U., Biodegradability study of active chitosan biopolymer films enriched with Quercus polyphenol extract in different soil types, Environmental Technology & Innovation. (2020). https://doi.org/10.1016/j.eti.2020.101318.

[6] Bajić, M., Ročnik, T., Oberlintner, A., Scognamiglio, F., Novak, U., Likozar, B., Natural plant extracts as active components in chitosan-based films: A comparative study, Food Packaging and Shelf Life. 21 (2019) 100365. 10.1016/j.fpsl.2019.100365.

[7] Bajić, M., Oberlintner, A., Kõrge, K., Likozar, B., Novak, U., Formulation of active food packaging by design: Linking composition of the film-forming solution to properties of the chitosan-based film by response surface methodology (RSM) modelling (2020). 10.1016/j.ijbiomac.2020.05.186.

[8] Rambabu, K., Bharath, G., Banat, F., Show, P. L., Cocoletzi, H. H., Mango leaf extract incorporated chitosan antioxidant film for active food packaging, International Journal of Biological Macromolecules. 126 (2019) 1234–1243. 10.1016/j.ijbiomac.2018.12.196.

[9] Hafsa, J., ali Smach, M., Ben Khedher, M. R., Charfeddine, B., Limem, K., Majdoub, H., Rouatbi, S., Physical, antioxidant and antimicrobial properties of chitosan films containing Eucalyptus globulus essential oil (2016). 10.1016/j.lwt.2015.12.050.

[10] Sánchez-González, L., González-Martínez, C., Chiralt, A., Cháfer, M., Physical and antimicrobial properties of chitosan-tea tree essential oil composite films (2010). 10.1016/j.jfoodeng.2010.01.026.

[11] Hromiš, N. M., Lazić, V. L., Markov, S. L., Vaštag, Ž. G., Popović, S. Z., Šuput, D. Z., Džinić, N. R., Velićanski, A. S., Popović, L. M.,

Optimization of chitosan biofilm properties by addition of caraway essential oil and beeswax (2015). 10.1016/j.jfoodeng.2015.01.001.

[12] Kõrge, K., Šeme, H., Bajić, M., Likozar, B., Novak, U., Reduction in Spoilage Microbiota and Cyclopiazonic Acid Mycotoxin with Chestnut Extract Enriched Chitosan Packaging : Stability of Inoculated Gouda Cheese, Foods. 9 (2020) 1645. 10.3390/foods9111645.

[13] Kõrge, K., Bajić, M., Likozar, B., Novak, U., Active chitosan–chestnut extract films used for packaging and storage of fresh pasta, International Journal of Food Science and Technology. 55 (2020) 3043–3052. 10.1111/ijfs.14569.

[14] Lavrič, G., Oberlintner, A., Filipova, I., Novak, U., Likozar, B., Vrabič-Brodnjak, U., Functional Nanocellulose, Alginate and Chitosan Nanocomposites Designed as Active Film Packaging Materials, Polymers. 13 (2021) 2523. 10.3390/polym13152523.

[15] Lepoittevin, B., Elzein, T., Dragoe, D., Bejjani, A., Lemée, F., Levillain, J., Bazin, P., Roger, P., Dez, I., Hydrophobization of chitosan films by surface grafting with fluorinated polymer brushes, Carbohydrate Polymers. 205 (2019) 437–446. 10.1016/j.carbpol.2018.10.044.

[16] Ahankari, S. S., Subhedar, A. R., Bhadauria, S. S., Dufresne, A., Nanocellulose in food packaging: A review, Carbohydrate Polymers. 255 (2021) 117479. https://doi.org/10.1016/j.carbpol.2020.117479.

[17] Bordenave, N., Grelier, S., Coma, V., Hydrophobization and antimicrobial activity of chitosan and paper-based packaging material, Biomacromolecules. 11 (2010) 88–96. 10.1021/bm9009528.

[18] Binsi, P. K., Ravishankar, C. N., Srinivasa Gopal, T. K., Development and Characterization of an Edible Composite Film Based on Chitosan and Virgin Coconut Oil with Improved Moisture Sorption Properties, Journal of Food Science. 78 (2013). 10.1111/1750-3841.12084.

[19] Niemczyk, A., Goszczyńska, A., Gołda-Cępa, M., Kotarba, A., Sobolewski, P., El Fray, M., Biofunctional catheter coatings based on chitosan-fatty acids derivatives, Carbohydrate Polymers. 225 (2019) 115263. https://doi.org/10.1016/j.carbpol.2019.115263.

[20] Miles, K. B., Ball, R. L., Matthew, H. W. T., Chitosan films with improved tensile strength and toughness from N-acetyl-cysteine mediated disulfide bonds, Carbohydrate Polymers. 139 (2016) 1–9. https://doi.org/10.1016/j.carbpol.2015.11.052.

[21] Mati-Baouche, N., Delattre, C., de Baynast, H., Grédiac, M., Mathias, J.-D., Ursu, A. V., Desbrières, J., Michaud, P., Alkyl-Chitosan-Based Adhesive: Water Resistance Improvement, Molecules. 24 (2019) 1987. 10.3390/molecules24101987.

[22] Piel, A., Plasma Generation, Springer Berlin Heidelberg, Berlin, Heidelberg, 2010, pp. 323–350. 10.1007/978-3-642-10491-6_11. URL https://doi.org/10.1007/978-3-642-10491-6{_}11

[23] Han, S., Lee, Y., Kim, Y.-W., Kim, Y., Chun, H., Lee, J., Plasma source ion implantation using high-power pulsed RF plasma, Surface and Coatings Technology. 186 (2004) 177–181. https://doi.org/10.1016/j.surfcoat.2004.04.045.

[24] Lu, F. X., Tang, W. Z., Huang, T. B., Liu, J. M., Song, J. H., Yu, W. X., Tong, Y. M., Large area high quality diamond film deposition by high power DC arc plasma jet operating at gas recycling mode, Diamond and Related Materials. 10 (2001) 1551–1558. https://doi.org/10.1016/S0925-9635(01)00407-1.

[25] Santos, C. A., Phuong, N. H., Park, M. J., Kim, S. B., Jo, Y. M., Decomposition of indoor VOC pollutants using non-thermal plasma with gas recycling, Korean Journal of Chemical Engineering. 37 (2020) 120–129. 10.1007/s11814-019-0406-8.

[26] Baranov, O., Bazaka, K., Kersten, H., Keidar, M., Cvelbar, U., Xu, S., Levchenko, I., Plasma under control: Advanced solutions and perspectives for plasma flux management in material treatment and

nanosynthesis, Applied Physics Reviews. 4 (2017) 041302. 10.1063/1.5007869.

[27] M. Santhosh, N., Filipič, G., Kovacevic, E., Jagodar, A., Berndt, J., Strunskus, T., Kondo, H., Hori, M., Tatarova, E., Cvelbar, U., N-Graphene Nanowalls via Plasma Nitrogen Incorporation and Substitution: The Experimental Evidence, Nano-Micro Letters. 12 (2020) 53. 10.1007/s40820-020-0395-5.

[28] Oberlintner, A., Shvalya, V., Vasudevan, A., Vengust, D., Likozar, B., Cvelbar, U., Novak, U., Hydrophilic to hydrophobic: Ultrafast conversion of cellulose nanofibrils by cold plasma fluorination, Applied Surface Science. (2022) 152276https://doi.org/10.1016/j.apsusc.2021.152276.

[29] Sheikhi, Z., Mirmoghtadaie, L., Abdolmaleki, K., Khani, M. R., Farhoodi, M., Moradi, E., Shokri, B., Shojaee-Aliabadi, S., Characterization of physicochemical and antimicrobial properties of plasma-treated starch/chitosan composite film, Packaging Technology and Science. 34 (2021) 385–392. 10.1002/pts.2559.

[30] Brodnjak, U. V., Jesih, A., Gregor-Svetec, D., Chitosan based regenerated cellulose fibers functionalized with plasma and ultrasound, Coatings. 8 (2018) 9–14. 10.3390/coatings8040133.

[31] Wanichapichart, P., Sungkum, R., Taweepreda, W., Nisoa, M., Characteristics of chitosan membranes modified by argon plasmas, Surface and Coatings Technology. 203 (2009) 2531–2535. https://doi.org/10.1016/j.surfcoat.2009.02.069.

[32] Wang, H., Fang, Y.-E., Yan, Y., Surface modification of chitosan membranes by alkane vapor plasma, J. Mater. Chem.. 11 (2001) 1374–1377. 10.1039/B009688L.

[33] Samanta, K. K., Amish G, J., Manjeet, J., Aswini K., A., Study of hydrophobic finishing of cellulosic substrate using He_1,3-butadiene plasma at atmospheric pressure _ Elsevier Enhanced Reader.pdf, Surface and Coatings Technology. 213 (2012) 65–76.

[34] Samanta, K. K., Gayatri, T. N., Saxena, S., Basak, S., Chattopadhyay, S. K., Arputharaj, A., Prasad, V., Hydrophobic functionalization of cellulosic substrates using atmospheric pressure plasma, Cellul. Chem. Technol.. 50 (2016) 745–754.

[35] Mauger, O., Westphal, S., Klöpzig, S., Krüger-Genge, A., Müller, W., Storsberg, J., Bohrisch, J., Plasma Activation as a Powerful Tool for Selective Modification of Cellulose Fibers towards Biomedical Applications, Plasma. 3 (2020) 196–203. 10.3390/plasma3040015.

[36] Samanta, K. K., Joshi, A. G., Jassal, M., Agrawal, A. K., Hydrophobic functionalization of cellulosic substrate by tetrafluoroethane dielectric barrier discharge plasma at atmospheric pressure, Carbohydrate Polymers. 253 (2021) 117272. https://doi.org/10.1016/j.carbpol.2020.117272.

[37] Chow, K. S., Khor, E., New flourinated chitin derivatives: synthesis, characterization and cytotoxicity assessment, Carbohydrate Polymers. 47 (2002) 357–363. https://doi.org/10.1016/S0144-8617(01)00190-4.

[38] Wijekoon, A., Fountas-Davis, N., Leipzig, N. D., Fluorinated methacrylamide chitosan hydrogel systems as adaptable oxygen carriers for wound healing, Acta Biomaterialia. 9 (2013) 5653–5664. https://doi.org/10.1016/j.actbio.2012.10.034.

[39] Cele, Z. E. D., Somboro, A. M., Amoako, D. G., Ndlandla, L. F., Balogun, M. O., Fluorinated Quaternary Chitosan Derivatives: Synthesis, Characterization, Antibacterial Activity, and Killing Kinetics, ACS Omega. 5 (2020) 29657–29666. 10.1021/acsomega.0c01355.

[40] Tabaght, F. E., El Idrissi, A., Aqil, M., Elbachiri, A., Tahani, A., Maaroufi, A., Grafting method of fluorinated compounds to cellulose and cellulose acetate: Characterization and biodegradation study, Cellulose Chemistry and Technology. 55 (2021) 511–528. 10.35812/CelluloseChemTechnol.2021.55.46.

[41] Ang, T.-F., Maiangwa, J., Salleh, A. B., Normi, Y. M., Leow, T. C.,

Dehalogenases: From Improved Performance to Potential Microbial Dehalogenation Applications, Molecules (Basel, Switzerland). 23 (2018) 1100. 10.3390/molecules23051100.

[42] Amorim, C. L., Carvalho, M. F., Afonso, C. M. M., Castro, P. M. L., Biodegradation of fluoroanilines by the wild strain Labrys portucalensis, International Biodeterioration & Biodegradation. 80 (2013) 10–15. https://doi.org/10.1016/j.ibiod.2013.02.001.

[43] Ojogbo, E., Blanchard, R., Mekonnen, T., Hydrophobic and Melt Processable Starch-Laurate Esters: Synthesis, Structure–Property Correlations, Journal of Polymer Science Part A: Polymer Chemistry. 56 (2018) 2611–2622. https://doi.org/10.1002/pola.29237.

[44] Wu, S., Surface and interfacial tensions of polymer melts. II. Poly(methyl methacrylate), poly(n-butyl methacrylate), and polystyrene, The Journal of Physical Chemistry. 74 (1970) 632–638. 10.1021/j100698a026.

[45] Liu, H., Adhikari, R., Guo, Q., Adhikari, B., Preparation and characterization of glycerol plasticized (high-amylose) starch–chitosan films, Journal of Food Engineering. 116 (2013) 588–597. https://doi.org/10.1016/j.jfoodeng.2012.12.037.

[46] Varma, R., Vasudevan, S., Extraction, Characterization, and Antimicrobial Activity of Chitosan from Horse Mussel Modiolus modiolus, ACS Omega. 5 (2020) 20224–20230. 10.1021/acsomega.0c01903.

[47] Aguirre-Loredo, R. Y., Rodríguez-Hernández, A. I., Morales-Sánchez, E., Gómez-Aldapa, C. A., Velazquez, G., Effect of equilibrium moisture content on barrier, mechanical and thermal properties of chitosan films, Food Chemistry. 196 (2016) 560–566. https://doi.org/10.1016/j.foodchem.2015.09.065.

[48] Leceta, I., Peñalba, M., Arana, P., Guerrero, P., de la Caba, K., Ageing of chitosan films: Effect of storage time on structure and optical, barrier and mechanical properties, European Polymer Journal. 66 (2015) 170–179. https://doi.org/10.1016/j.eurpolymj.2015.

02.015.

[49] Allison, C. L., Lutzke, A., Reynolds, M. M., Identification of low molecular weight degradation products from chitin and chitosan by electrospray ionization time-of-flight mass spectrometry, Carbohydrate Research. 493 (2020) 108046. https://doi.org/10.1016/j.carres.2020.108046.